

SECRET

UNCLASSIFIED

LAMS-2919

C.3

Copy No. [REDACTED]

**CIC-14 REPORT COLLECTION
REPRODUCTION
COPY**

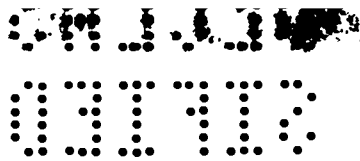
**LOS ALAMOS SCIENTIFIC LABORATORY
OF THE UNIVERSITY OF CALIFORNIA ○ LOS ALAMOS NEW MEXICO**

**INVESTIGATIONS OF UNDERGROUND EXPLOSIONS
IN NEVADA SANDY SOIL
(Title Unclassified)**

LOS ALAMOS NATIONAL LABORATORY
3 9338 00362 4748

[REDACTED]

UNCLASSIFIED



LEGAL NOTICE

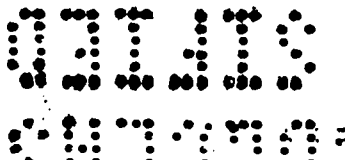
This report was prepared as an account of Government sponsored work. Neither the United States, nor the Commission, nor any person acting on behalf of the Commission:

A. Makes any warranty or representation, expressed or implied, with respect to the accuracy, completeness, or usefulness of the information contained in this report, or that the use of any information, apparatus, method, or process disclosed in this report may not infringe privately owned rights; or

B. Assumes any liabilities with respect to the use of, or for damages resulting from the use of any information, apparatus, method, or process disclosed in this report.

As used in the above, "person acting on behalf of the Commission" includes any employee or contractor of the Commission, or employee of such contractor, to the extent that such employee or contractor of the Commission, or employee of such contractor prepares, disseminates, or provides access to, any information pursuant to his employment or contract with the Commission, or his employment with such contractor.

UNCLASSIFIED



UNCLASSIFIED

UNCLASSIFIED

~~CONFIDENTIAL~~
SECRET

PUBLICLY RELEASABLE

Per M Jones FSS-16 Date: 10-6-95
By Kolar CIC-14 Date: 10-20-95

LAMS-2919

This document consists of 30 pages

No. 10 of 10 copies, series _____

LOS ALAMOS SCIENTIFIC LABORATORY
OF THE UNIVERSITY OF CALIFORNIA LOS ALAMOS NEW MEXICO

REPORT WRITTEN: January 15, 1962

REPORT DISTRIBUTED: August 12, 1963

VERIFIED UNCLASSIFIED

Per EMS 6-20-79
By Kolar 10-20-95

INVESTIGATIONS OF UNDERGROUND EXPLOSIONS
IN NEVADA SANDY SOIL
(Title Unclassified)

by

Kenneth H. Olsen

Classification changed to UNCLASSIFIED
by authority of the U. S. Atomic Energy Commission,

Per Jack H. Rohrer, Chief, Adm. Serv. Div. AEC, Wash. 2-15-72
By REPORT LIBRARY New Law 5-23-72

Contract W-7405-ENG. 36 with the U. S. Atomic Energy Commission

All LAMS reports are informal documents, usually prepared for a special purpose and primarily prepared for use within the Laboratory rather than for general distribution. This report has not been edited, reviewed, or verified for accuracy. All LAMS reports express the views of the authors as of the time they were written and do not necessarily reflect the opinions of the Los Alamos Scientific Laboratory or the final opinion of the authors on the subject.

~~RESTRICTED DATA~~

~~...the disclosure of its contents in any manner to an unauthorized person is prohibited.~~

UNCLASSIFIED

Group 1 - Excluded from automatic
downgrading and declassification
APPROVED FOR PUBLIC RELEASE

GROUP 1
EXCLUDED FROM AUTOMATIC
DOWNGRADING AND DECLASSIFICATION



UNCLASSIFIED

CONFIDENTIAL

UNCLASSIFIED

CONFIDENTIAL

LAMS-2919

AEC Classified Technical Library
Lawrence Radiation Laboratory, Livermore
Manager, ALO (Paul Ager)
Los Alamos Report Library

1-3
4
5
6-40

UNCLASSIFIED

CONFIDENTIAL

UNCLASSIFIED

CONFIDENTIAL
APPROVED FOR PUBLIC RELEASE

UNCLASSIFIED

SECRET

I INTRODUCTION

This report presents further information on blast calculations carried out with the J-15 Lagrangian radiation-diffusion hydrodynamics code. Here we deal primarily with explosions in Nevada alluvium. The purpose of these calculations is to determine total bomb yields from observed shock pressures and arrival times.

In order to make these calculations, we require the initial configuration and the equations of state of the materials involved. The following simplifying assumptions have been made:

1. The soil is assumed to be homogeneous.
2. Spherical symmetry is assumed. Although the bomb chamber is certainly not a sphere, the bomb mass and chamber dimensions are usually small as compared with the mass of the soil and the shock radii at the ranges of interest. In this case, the exact properties of the explosion chamber and materials can be expected to have only slight effects on the time history of the shock expansion in the soil.
3. The material is assumed to be fluid with no shear stresses.
4. The equation of state of desert alluvium is taken to be of the Mie-Grüneisen type below the melting point:

UNCLASSIFIED

SECRET

UNCLASSIFIED

.
 01110
 01110

$$P = P_H + \frac{\gamma_G(V)}{V} (E - E_H). \quad (1)$$

Here P is the pressure, V is the specific volume, and E the specific internal energy. For a given phase, the empirical relationship between the shock velocity U_s and the particle velocity U_p is found to be

$$U_s = c + s U_p. \quad (2)$$

Combining (2) with the Rankine-Hugoniot relations gives

$$P_H = \frac{c^2(V_0 - V)}{[V_0 - s(V_0 - V)]^2} \quad (3)$$

and

$$E_H = \frac{P_H(V_0 - V)}{2}. \quad (4)$$

All changes after shock passage are assumed to be adiabatic giving

$$E = - \int_{V_0}^V P dV. \quad (5)$$

V_0 is the specific volume under ambient conditions.

Above the melting point, a gaseous equation of state is used.

This is based on a Thomas-Fermi-Dirac atomic model calculated by R. D. Cowan with low pressure corrections calculated in J-15 using the Saha ionization equation.

We shall now proceed to a more detailed discussion of the basic quantities c , s , and γ .

01110

UNCLASSIFIED

01110
 01110

UNCLASSIFIED

II EQUATION OF STATE PARAMETERS

A. GMX-6 Data.

R. G. McQueen of GMX-6 has measured the Hugoniot of two samples of Nevada alluvium furnished by J-15 (LAMS-2760). The samples were very friable, and it was impossible for GMX-6 to machine specimens suitable for their shots. As an alternative, the samples were broken up, damp packed into the base plates, and dried before shooting. The two samples were considerably different as regards particle size distribution, the coarser aggregate having a dry density of 1.80 gm/cc and the finer aggregate having a density of 1.54 gm/cc. The results of the experiments are shown in the U_s , U_p plane in figure 1. The shock pressures are listed alongside of the observed U_s , U_p points.

We have taken the in situ density in Area Three at NTS to be 1.7 gm/cc for lack of a more accurate number; the solid line in figure 1 represents the U_s versus U_p curve for this ambient pre-shot density. For many solids in certain shock stress ranges, the shock velocity U_s may be less than the sound velocity in the unstressed material. Shocks of these strengths will therefore travel at less than the ambient sound speed and will be preceded by a sonic "elastic precursor." Sonic surveys made in Nevada are somewhat uncertain, but indicate sonic velocities of the order of 1.5 km/sec. The GMX-6 data extrapolate to 0.55 km/sec, and we would hence expect to see a two wave structure below shock pressures of about 15 kilobars if the dynamic yield strength of the material is taken to be 1 kilobar. A sonic precursor of this strength is expected to trigger the timing indicators during the expansion of the shock so that the more distant stations will see the elastic precursor rather than the main shock.

UNCLASSIFIED

UNCLASSIFIED

0130
0704

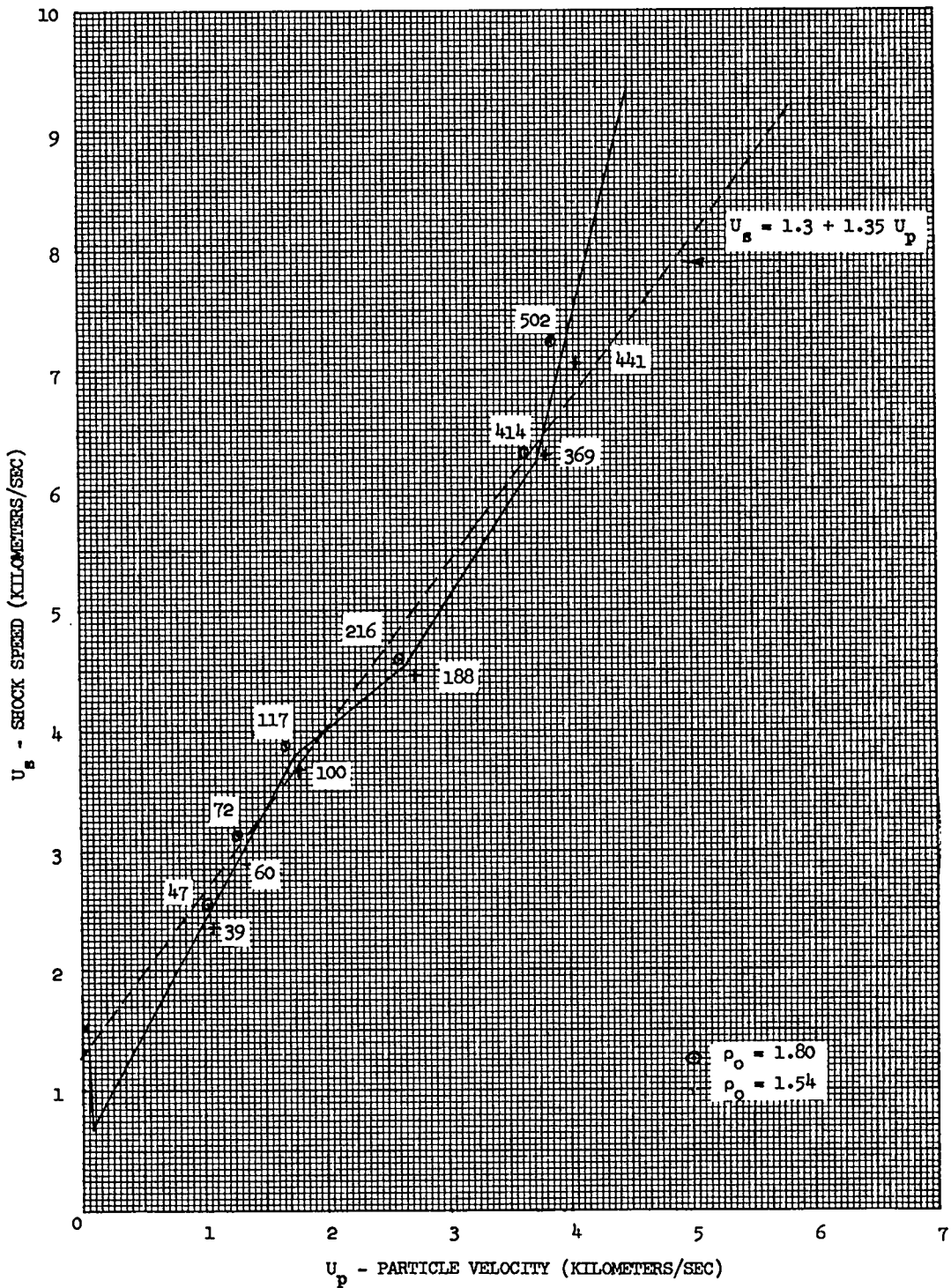


Figure 1

0130

0704

UNCLASSIFIED

UNCLASSIFIED

SECRET

SECRET

Preliminary information from the Fisher event indicates that the ambient sound speed should perhaps be as low as 1 km/sec in which case the two wave structure should develop below about 5 kilobars. Figure 1 shows only the elastic precursor for an ambient sound velocity of 1.5 km/sec.

According to McQueen, the break in the U_s versus U_p curve between 100 and 200 kilobars is a mixed phase region which is almost certainly associated with a similar transition observed in granite at higher pressures. Above about 400 kilobars, the slope of the curve is such that the volume increases with increasing pressure. We have chosen to interpret this as an indication that the alluvium melts at about 400 kilobars. In any case, the J-15 numerical integrations are unstable under this type of situation, and we have chosen to extrapolate the phase line between 200 and 400 kilobars until we reach our specified melting temperature at which time we switch to our gaseous equation of state.

Although the GMX-6 data clearly indicate at least three phase regions of interest, the best single straight line fit of the data is

$$U_s (\text{km/sec}) = 1.3 + 1.35 U_p . \quad (6)$$

In order to evaluate some of the uncertainties in the calculation, several problems were run with equation 6 as well as a more complete set of problems with the multiphase Hugoniot.

In summary, the GMX-6 data define the Hugoniot of Nevada alluvium reasonably well below 400 kilobars. For yields of the order of 10 kilotons and the present layout of measuring stations in Area Three, the region above 400 kilobars is not of great importance for time of arrival measurements. This is because the mass and volume of soil shocked to such pressures is relatively small and would be expected to have only minor effects on time of arrival at the more distant stations.

SECRET

SECRET

UNCLASSIFIED

.

0313

The most important pressure for the J-15 integrations is below about 50 kilobars; test problems indicate that the peak shock pressures drop below 50 kilobars at ranges of about 10 to 15 meters (for 10 KT). Since this (40-50 kb) is about the minimum pressure obtainable in the GMX-6 type experiments, it is worthwhile to verify that the extrapolation of the GMX-6 data to zero pressure is reasonable. Ideally, the best method for doing this would be to make simultaneous measurements of both time of arrival and peak pressure at every measuring station for the full scale nuclear shot. Time of arrival measurements would give the shock speed, U_s , at each station; and the pressure measurement, when combined with the Rankine-Hugoniot condition,

$$P = \rho_0 U_s U_p, \quad (7)$$

could be used to calculate U_p . From these data, the U_s versus U_p curves could then be constructed.

Unfortunately, the first few shots of the Nougat-Ivanhoe series have not been instrumented for pressure measurements at every range station, although it is hoped that the later shots will include at least some of these measurements. It is not now known if these in situ pressure measurements will have the precision necessary to give a well determined U_s versus U_p curve for each shot, but if they could be made sufficiently accurate, such a technique would eliminate several of the present uncertainties in the equation of state. The most obvious advantage of this method would be the elimination of the present assumption that the data obtained by GMX-6 is typical of all the material in which the Nougat-Ivanhoe shots are to be made. The method would also help answer the question of whether the

0313

0313

0 1 2 3 4
 5 6 7 8 9

technique of repacking the samples as done by GMX-6 really approximates the material packing at depth in Nevada.

B. CMF-5 Data.

Since the in situ method of measuring the Hugoniot of Nevada alluvium as discussed above has not yet been performed or may not be of sufficient accuracy in the future, an attempt was made to verify the extrapolation of the GMX-6 data below 40 kilobars by making static pressure-volume measurements on the samples of alluvium obtained from Nevada. The work was kindly undertaken for us by Karl Gschneidner of CMF-5 who has a press capable of attaining pressures up to 10 kilobars.

The idea of the experiment is to obtain the average bulk properties of the mineral grains, neglecting effects due to voids between the grains and the fracturing of grain edges and corners. The experimental technique was to measure the grain density and then to introduce a slurry of grains and glycerin into the pressure cell. The glycerin acts as a pressure transmitting fluid around the individual grains and also excludes the air voids. Corrections were made for the effects of the glycerin component on the observed compressibilities.

The results of Gschneidner's measurements are shown in figure 2, where the reference density is taken as the average observed grain density (2.16 gm/cc). The sample was first compressed to about 10 kb (Run 1), the pressure relieved and again compressed to 10 kb (Run 2). Note the divergence of the two runs at the higher pressures. A possible explanation of this divergence may be that the sample grains may still be somewhat porous and that the first application of pressure forced glycerin into these pores thus making the material "harder" when it was recompressed. The consequences of this hypothesis will be discussed in more detail below.

0 1 2 3 4
 5 6 7 8 9

03715

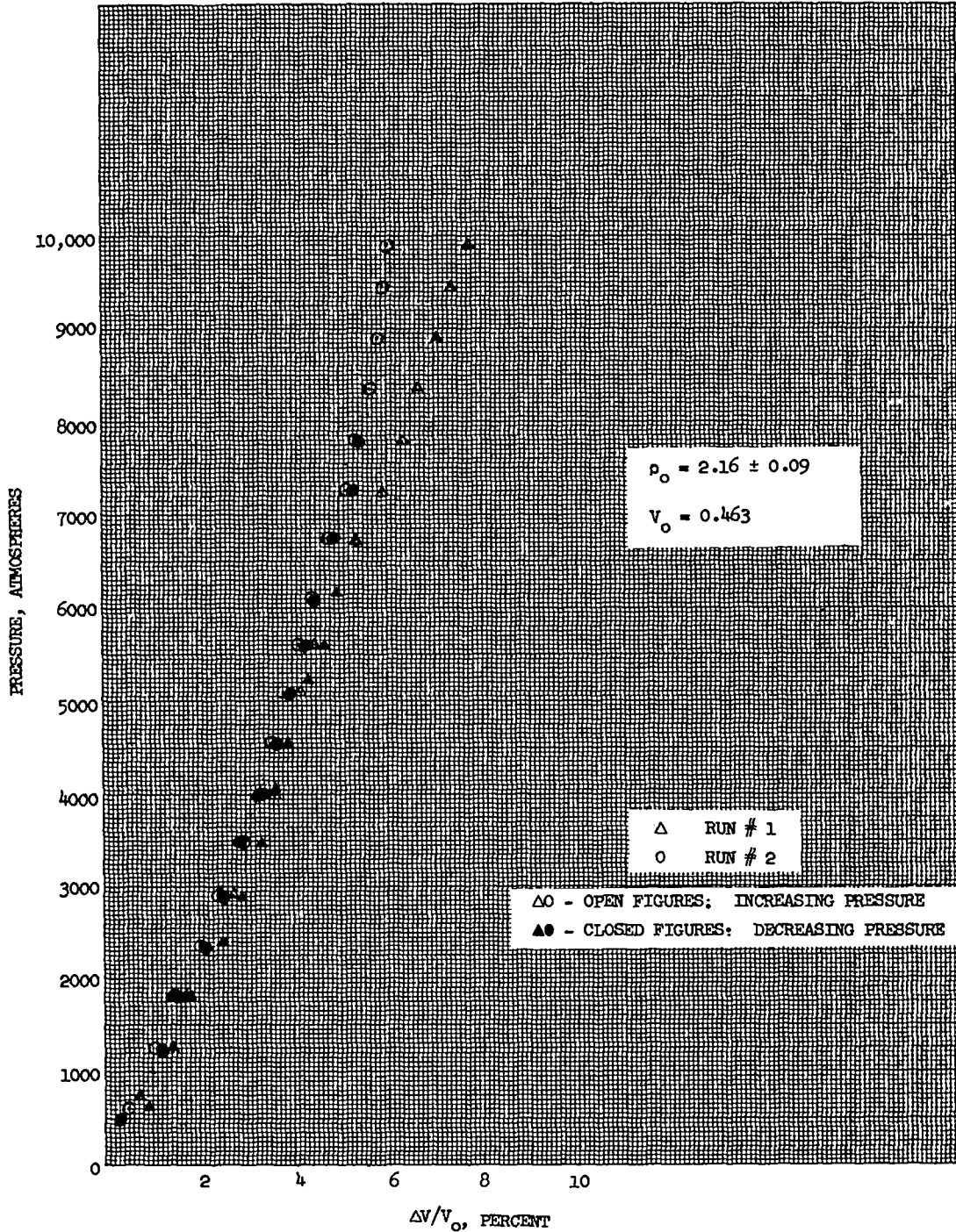


Figure 2
(CMF-5 Data)

03715
03715

CONFIDENTIAL

The CMF-5 points must be corrected to a reference density of 1.7 gm/cc in order to compare them with the extrapolated GMX-6 data. This was done by solving for the specific volume using Gschneidner's observed grain density of 2.16 gm/cc and then recomputing the relative volume change with a reference density of 1.7 gm/cc. The points were transferred to a U_s versus U_p plot by making use of two of the Rankine-Hugoniot conservation equations:

$$\frac{U_p}{U_s} = 1 - \frac{V}{V_0} \quad (8)$$

$$U_s^2 = \frac{P V_0}{\left(1 - \frac{V}{V_0}\right)} \quad (9)$$

Here V_0 is the reciprocal density, $V_0 = 0.588 = 1/1.7$. The results of these transformations of the CMF-5 data are shown in figure 3 together with the extrapolated line from the GMX-6 shots. It will be noted that the static measurements reduced in the above manner fall reasonably close to the extrapolated line, but that the indicated slope is greater than the expected value of 1.85. On the other hand, the bulk sonic speed calculated from the initial slope of the CMF-5 P-V curve gives an intercept of about 0.52 km/sec after making the density correction noted above. This is in quite good agreement with the value of 0.55 km/sec obtained from the extrapolation of the dynamic data. If we accept the idea that the mineral grains were somewhat porous and that the effect of the glycerin entering these pores on compression was to make the material harder to compress, a steeper slope in the U_s versus U_p would be expected. As a test of this effect, the $\Delta V/V_0$ points from figure 2 were multiplied by a constant factor of 2 in the range 3 to 10 kb and the reference density correction made to these "adjusted"

CONFIDENTIAL

CONFIDENTIAL

00710

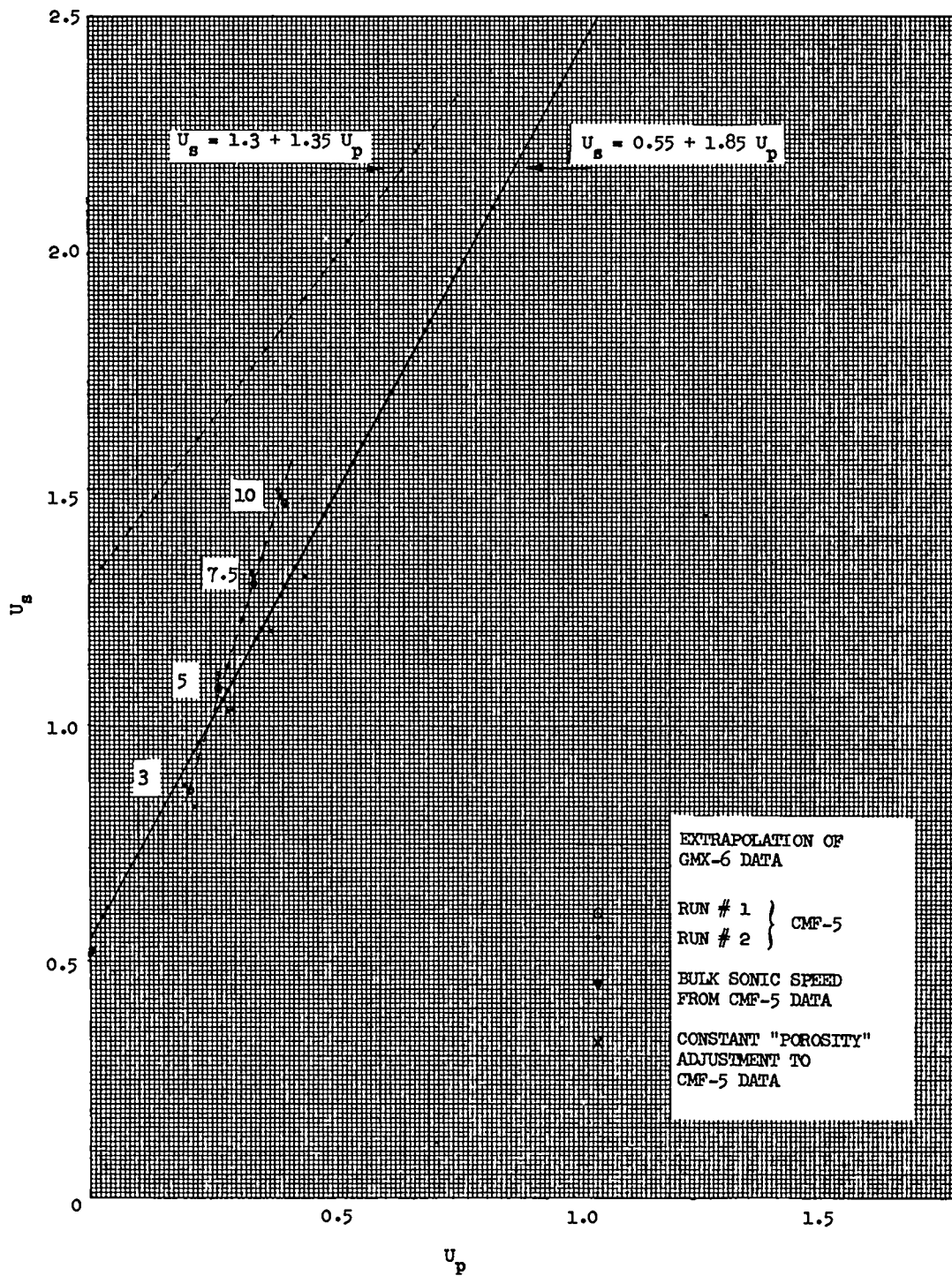


Figure 3

00710

00710

U. S. G. O.



values. The results are shown as crosses in figure 3. It is seen that such an adjustment brings the CMF-5 data more nearly into agreement with the extrapolation of the dynamic GMX-6 data, although the constant factor of 2 used seems to be an overcorrection, especially for the lower pressures. In any case, the static experiments indicate that the low pressure (below 100 kb) Hugoniot follows more nearly the relation

$$U_s = 0.55 + 1.85 U_p \quad (10)$$

rather than a curve similar to equation 6. Although we cannot at present rule out the possibility that the static measurements may indicate the existence of different phase region than that given by equation 10, the indications are that the difference in slope may be explained by the effects of porous grains in the static measurements. Until further information is available, it seems reasonable to use equation 10 down to pressures at which the sonic precursor is effective.

C. Grüneisen Ratio.

In addition to the quantities c and s , another important parameter in our equation of state is the Grüneisen ratio, γ_G . The size of γ_G determines how rapidly the pressure falls off behind the shock and hence is effective in determining the expansion rate of the shock front as well as the amount of cooling in the adiabatic expansion. There are several methods for estimating the size of this parameter:

1. For many metals, the Dugdale-MacDonald relation (cf., McQueen and Marsh J.A.P., 31, 1253 1960) has been found to be generally accurate to within about 35%. This relation yields

the formula

$$\frac{U_s}{U_p} = 1 + \frac{\gamma_G}{2} \frac{U_p}{c}$$

U. S. G. O.

01113
03113

$$\gamma_G = \frac{V}{V_0} \left[s^2 - \frac{1}{3}s + \frac{5}{9} \right] - s^2 + \frac{7}{3}s - \frac{14}{9} . \quad (11)$$

At zero pressure ($V/V_0 = 1$) equation 11 reduces to

$$\gamma_0 = 2s - 1 , \quad (12)$$

so that γ_G may be obtained directly from the observed U_s versus U_p curve. For our observed s of 1.85, equation 12 gives $\gamma_G = 2.7$ at zero pressure.

2. The value of γ at room temperature and pressure may be computed by the thermodynamic identity

$$\gamma_T = V \left(\frac{\partial P}{\partial E_V} \right) = \frac{V\alpha}{Kc_V} = \frac{\alpha c^2}{c_P} \quad (13)$$

and the measured quantities:

c = adiabatic bulk sound speed

α = volume coefficient of expansion = $\frac{1}{V} \left(\frac{\partial V}{\partial T} \right)_P$

K = isothermal compressibility = $-\frac{1}{V} \left(\frac{\partial V}{\partial P} \right)_T$

c_P = specific heat at constant pressure

c_V = specific heat at constant volume

Table I, compiled by Stan Marsh from available handbook data on common igneous rocks gives a comparison of γ_0 computed from equation 13 and also from equation 12. Note that for most rocks, equation 13 gives a considerably smaller γ than does equation 12. This tends to cast some doubt on the applicability of the Dugdale-MacDonald relation to rocks.

14 01113

03113

Table I

Material	ρ_o gm/cm ³	C cm/sec	S	α /°C	C_p ergs/gm/°C	γ_o $(\frac{\alpha C^2}{C_p})$	γ_o (2S-1)
Dunite	3.32	6.6 x 10 ⁵	.88	33.8 x 10 ⁻⁶	10 ⁷	1.47	.76
Dunite	3.32	6.15	1.0	33.8	"	1.28	1.0
Dunite	3.8	5.93	1.0	33.8	"	1.19	1.0
Pyroxene	3.30	5.88	1.0	16	"	.55	1.0
Pyroxene	3.28	6.1	1.0	16	"	.60	1.0
Dunite	3.8	4.95	1.15	33.8	"	.83	1.30
Pyroxene	3.28	5.28	1.15	16	"	.45	1.30
Pyroxene	3.30	4.57	1.375	16	"	.33	1.75
Diabase	3.0	3.47	1.47	16.2	"	.20	1.94
Albitite	2.61	2.83	1.47	12	"	.096	1.94
Anorthosite	2.75	3.0	1.47	15	"	.14	1.94
Diabase	3.0	5.3	1.0	16.2	"	.46	1.0
Granite	2.61	4.6	1.0	24	"	.51	1.0

APPROVED FOR PUBLIC RELEASE

APPROVED FOR PUBLIC RELEASE

.
 0110

Equation 13 was used to estimate γ for Nevada alluvium by assuming the specific heats given by the Dulong-Petit law, the thermal expansion coefficient of granite and the observed intercept of the U_g versus U_p curve which is confirmed by the CMF-5 measurements. This estimate gives a value of γ_T of the order of 0.01. The greatest uncertainty in this computation is the value of the thermal expansion coefficient α . It may be argued that instead of the granite value, a more reasonable α to use would be a value of the order of that for an ideal gas because of the large volume of air entrapped in the sedimentary alluvium. Since α for a gas is about two orders of magnitude larger than that for granite, a value of about unity would then be obtained for γ .

3. The third Rankine-Hugoniot equation can be written

$$E_H - E_O = \frac{1}{2}(P_H + P_O)(V_O - V). \quad (14)$$

where zero subscripts refer to the ambient state. If the material is available at two different initial densities and these are both shocked to the same final density, the pressures and energies will therefore be different. This fact may be used to compute Grüneisen's ratio directly from the shock measurements of the two samples by the equation

$$\gamma_G = v \left(\frac{\Delta P}{\Delta E} \right) \simeq 2v \left[\frac{P_{H2} - P_{H1}}{[(P_{H2} + P_{O2})(V_{O2} - V) - (P_{H1} + P_{O1})(V_{O1} - V)]} \right]. \quad (15)$$

016
 0110

0110
 0110

SECRET
SECRET

Such an experimental procedure for iron has recently been reported in the Russian literature (Al'tshuler et al. Soviet phys JETP 34, 606, 1958). Since the GMX-6 shots were made on two repacked samples of different densities, this procedure was used to obtain yet another estimate of γ_G . Inspection of the Hugoniot curves measured by GMX-6 (see figure 5 on page 13 of LAMS-2760) showed that the only region in which the two Hugoniots were simultaneously well determined at a single density was in the vicinity of a density of 3.0 gm/cc. Application of equation 15 gave a γ_G of about 1.5 to 1.7. Equation 11 gives a value of 1.25 at this compression. The sketched in curves in LAMS-2760 at a density of 3.8 gm/cc give a γ_G of about 0.58 whereas application of equation 11 yields 0.25. This point is of questionable validity because the material is in the mixed phase region at this compression.

In view of these estimates, it seems probable that γ lies somewhere between 0.5 and 2 with a value of about 1 being a reasonable compromise. A constant Grüneisen ratio of 0.5 has been used in many of the problems that have been run to date and gives the slope of the radius time curve for Fisher shot much better than $\gamma_G = 1.5$. We conclude that equation 11 is of questionable validity especially when the material behind the shock has expanded greatly thus giving very large γ_G . We are at present inclined to use a constant γ_G rather than the variable form indicated by equation 11.

SECRET

SECRET

U. S. G. O.
 DIVISION

The code has provision for including latent heats of fusion and of vaporization at the melting and vaporization temperatures respectively. Since these quantities are very poorly known for many minerals and not measured for Nevada alluvium they are usually set to zero in our calculations. In addition, finite latent heats complicate our integrations by introducing instabilities which damp out slowly in the melted region. In any case, the effects on the arrival time appear to be only important at ranges considerably closer to the bomb than the closest station in the present layout.

Somewhat similar instabilities occur when a zone, once melted, cools by expansion below the melting point. If the "resolidified" zone is allowed to change back from a TFD equation of state to a Grüneisen type equation of state, an instability is set up and the time interval used in the integration must be temporarily reduced in order to allow the instability to damp out. If the zone is forced to always use the gaseous TFD equation after melting on compression and not allowed to change back to the Grüneisen equation after the expansion, the problems run much more rapidly and fewer instabilities occur. Since the shock has progressed a considerable distance in the solid by the time the melted region cools again to the melting point, the continued use of the gaseous TFD equation in the inner zones does not have much effect on the radius versus time curves for the later stages of the expansion, except to make the problem easier to run on the machine. As an example, two problems were run at 13 kilotons and a constant γ_G of .01. Melted zones in problem 65 were allowed to resolidify to the Grüneisen equation of state, whereas the same zones in problem 68 were forced to retain the gaseous equation of state. At 8 milliseconds the shock radius for problem 65 was 23.2 meters and that

U. S. G. O.
 DIVISION

U. S. G. O.
 DIVISION

.
 01110

for problem 68 was about 23.5 meters. Comparing problem 63, run at 10 kilotons we have $R_g = 22.0$ m at 8 ms. Thus the error introduced by not allowing resolidification appears to be worth the equivalent of about 1 kiloton at yields in the 10 to 15 kt range. Since we do not expect accuracies much better than about 30% for yield measurements by this method, we have chosen to retain the gaseous equation of state once a zone has melted, and not change back to the Grüneisen equation on expansion.

The numerical integrations are reasonably insensitive to the size of the zoning used in setting up the problems. The usual zoning scheme is to assign the first zone (bomb chamber) a radius of 1 meter; each successive alluvium zone is assigned a radius such that its mass is about a factor of 2 above the mass of the preceding zone. This factor of 2 is applied until the difference in radii of two successive zones is about 2 meters (for yields in the vicinity of 10 kilotons) and thereafter a constant ΔR of 2 meters is maintained. For yields of the order of 1 or 2 kt, the maximum ΔR allowed is 1 meter or less. An even finer mesh would be desirable in order to more accurately locate the shock front within a zone but the above prescription seems to be adequate for most purposes. To see the effects of zoning changes, problem 61 run with the first zone radius at 5 meters (using alluvium equation of state rather than iron) may be compared with problem 79 in which the first zone had $R_0 = 1$ meter and used the iron equation of state for that zone. Both problems were run at 10 kt and used a variable γ_G (equation 11). Problem 61 gives shock radii greater than problem 79 by about 0.5 meter for times greater than 3 or 4 milliseconds. Problem 61 also had maximum zone widths of about 3.5 meters whereas the maximum for problem 79 was 2 meters. Such a zoning

0201110

01110

ALLIUM
 DTIC

difference is extreme and we expect the error in our integrations due to zoning differences to be less than the equivalent of 1 kt in the 10 kt range.

A variation in the assumed density of the first zone (bomb chamber) has fairly small effects. A change in assumed density of 1.7 gm/cc (problem 72) to 1.0 gm/cc (problem 73) gives a difference in shock radii of about 2% at 4 milliseconds. Both problems were run at 1 kiloton and a constant $\gamma_G = 0.5$.

We are at present using a melting point of 0.5 volt (5800°K) for alluvium. It is very likely that this is too high. However, Cowan's TFD equations are not expected to be reliable below temperatures of 1 volt and in fact sometimes give negative pressures below 0.5 volts. Hence the uncertainties in the Cowan tables below temperatures of 1 volt force us to make a choice of a melting point that is not too low. We believe that the break in the U_g versus U_p curve at about 400 kilobars (figure 1) is an indication of melting. Nuckolls of LRL also states that tuff melts on being shocked to about 400 kilobars (see UCRL 5675, page 123). If we accept a melting point of 0.5 volt we find from our listings that alluvium reaches this temperature by being shocked to pressures between about 340 and 500 kilobars depending on the assumed Grüneisen's ratio. For $\gamma_G = 0.5$ the pressure reaches 340 kb just prior to melting and for $\gamma_G = 4.5$, a pressure of 490 kb is present just below the melting temperature. In any case, a fairly large change in the assumed melting points does not seem to affect the computed radius versus time curves. As an example, problem 78 (melting temperature = 1 volt) and problem 79 (melting temperature = .5 volt) show a negligible difference in the shock radius (20.5 meters) at 5 milliseconds. Both problems were run at 10 kilotons.

ALLIUM
 DTIC

.

Although the shock radius versus time curves do not seem to be very sensitive to the assumed melting points, the computation of the size of the melted region and the subsequent cavity would show a greater sensitivity. In view of possible interest in estimating the cavity size, some further discussion of the proper melting temperatures will be made here.

As far as we are aware, no extensive experimental work has been done on the variation of melting point with pressure for various minerals and rocks. Various theoretical estimates for the melting points and temperatures for minerals in the earth's deep interior are reviewed by Verhoogen (in Physics and Chemistry of the Earth. Volume 1, 1956) and by Gutenberg (Physics of the Earth's Interior). We shall summarize the theory briefly below.

The increase of melting point T^* with pressure P for a given phase of the material is given by the Clapeyron equation

$$\frac{dT^*}{dP} = \frac{\Delta V}{\Delta S} = \frac{\Delta V}{(L/T^*)} \quad (16)$$

where $\Delta V/\Delta S$ is the ratio of the volume change to the entropy change at the melting point, L is the latent heat of fusion. Some information on latent heats and volume changes for minerals at atmospheric pressure are given in the Handbook of Physical Constants (Geological Society of America Special Paper No. 36 - edited by F. Birch). Verhoogen (page 26) quotes the following experimental values for the initial slope of the melting point curve in degrees per kilobar: Fosterite 4.7; diopside 13; albite, 26. Jefferies (The Earth, 4th edition, page 288) adopts as "fairly typical values for silicate rocks:"

$$T_0^* = 1300^\circ\text{K}, L = 100 \text{ cal/gm}, \frac{\rho(\text{liquid})}{\rho(\text{solid})} = 0.9$$

.

.

U.S. GOVERNMENT
PRINTING OFFICE

If ρ_s is taken to be of the order of 3 gm/cc for these "typical minerals", we get $dT^*/dp \cong 10^\circ\text{K}/\text{kilobar}$. A value of $dT^*/dp = 10^\circ\text{K}/\text{kilobar}$ would give a melting point of $\sim 5500^\circ\text{K}$ at 400 kb if we assume the "melting point" of alluvium is approximately 1500°K .

Unfortunately, the slope of the melting point curve is expected to decrease appreciably at higher pressures because ΔV becomes smaller (the compressibility of the liquid is usually higher than that for the corresponding solid). According to Verhoogen, Δs is not likely to be very much affected by increasing pressure. Thus, melting points estimated on the basis of the initial slope alone are likely to be too high.

Simon has experimentally studied the change in melting point under pressure for substances (eg. helium) with very low melting points and which can be investigated over a wide range of pressure. He finds that these substances obey the law

$$\frac{P}{\alpha} = \left(\frac{T^*}{T_0^*} \right)^c - 1. \quad (17)$$

Here T^* is the melting point at pressure P , T_0^* the melting point at zero pressure, c is a constant and α is related to the "internal pressure", $-(\partial E/\partial V)_T$. Simon has used equation 17 to estimate the melting point of iron under high pressure (Nature, 172, 746, 1953).

Combining equations 16 and 17 we find

$$\alpha c = \frac{L}{\Delta V}. \quad (18)$$

Simon finds that $\alpha/(\partial U/\partial V)_T = 1.5$ from the data on alkali metals and assumes this to hold for other materials. The constant, α , may be estimated from the melting point at zero pressure by

U.S. GOVERNMENT
PRINTING OFFICE

U.S. GOVERNMENT
PRINTING OFFICE

.

0110

$$\left(\frac{\partial E}{\partial V}\right)_T = \gamma_G \frac{c_V T_O^*}{V}; \quad (19)$$

where c_V is the specific heat, V the specific volume and γ_G is our old friend, Grüneisen's ratio.

Applying Simon's formula to various estimates of the initial slope of the melting point curve we arrive at Table II as estimates of the melting temperatures at a pressure of 400 kilobars. The melting point at atmospheric pressure for alluvium was assumed to be 1500°K in these computations. Case c corresponds to Nuckolls' estimate of a latent heat of fusion of 715 calories/gm for Tuff (UCRL 5675, Page 123), an assumed density of 1.7 gm/cc and a volume change of 10% on melting.

In view of the extreme uncertainty in the basic data entering into the computations listed in Table II, we cannot rule out a melting point as high as 5800°K, but it seems more likely that it is not over about 2500°K at 400 kb. Until our gaseous TFD equation of state is adjusted to give better results at low temperature, we have chosen to retain the 5800° figure.

IV RESULTS AND CONCLUSIONS

Some of the computed shock radius versus time curves are summarized in figures 4, 5 and 6. They show the sensitivities to various assumed parameters. The curves are the best smooth curves as determined from the individual shock radii given by the listings.

Figure 4 shows the difference between equation 6 and the three phases defined by the constants:

$$\begin{aligned} c_0 &= 0.55 \text{ m/ms}, s_0 = 1.85, \text{ valid for } V > 0.317 \text{ cm}^3/\text{gm} \\ c_1 &= 2.40 \text{ m/ms}, s_1 = 0.80, \text{ valid for } 0.317 > V > 0.242 \\ c_2 &= 0.2 \text{ m/ms}, s_2 = 1.62, \text{ valid for } 0.242 > V. \end{aligned} \quad (20)$$

24.0110

0110

Table II

$$\left(\frac{dT^*}{dP}\right)_{P=0} \left(\frac{^{\circ}K}{Kb}\right)$$

T* at P = 400 kb

	α_c (kilobars)	α (kilobars)	c	T* at P = 400 kb		
				$\gamma_G = 0.5$	$\gamma_G = 1.0$	
A	10	150	$\sim 25 \gamma_G$	$\sim 6/\gamma_G$	2000°K	2400°K
B	30	50	$\sim 25 \gamma_G$	$\sim 2/\gamma_G$	3600°K	6300°K
C	3	500	$\sim 25 \gamma_G$	$\sim 20/\gamma_G$	1640°K	1730°K

APPROVED FOR PUBLIC RELEASE

A
B
C

APPROVED FOR PUBLIC RELEASE

APPROVED FOR PUBLIC RELEASE

SECRET

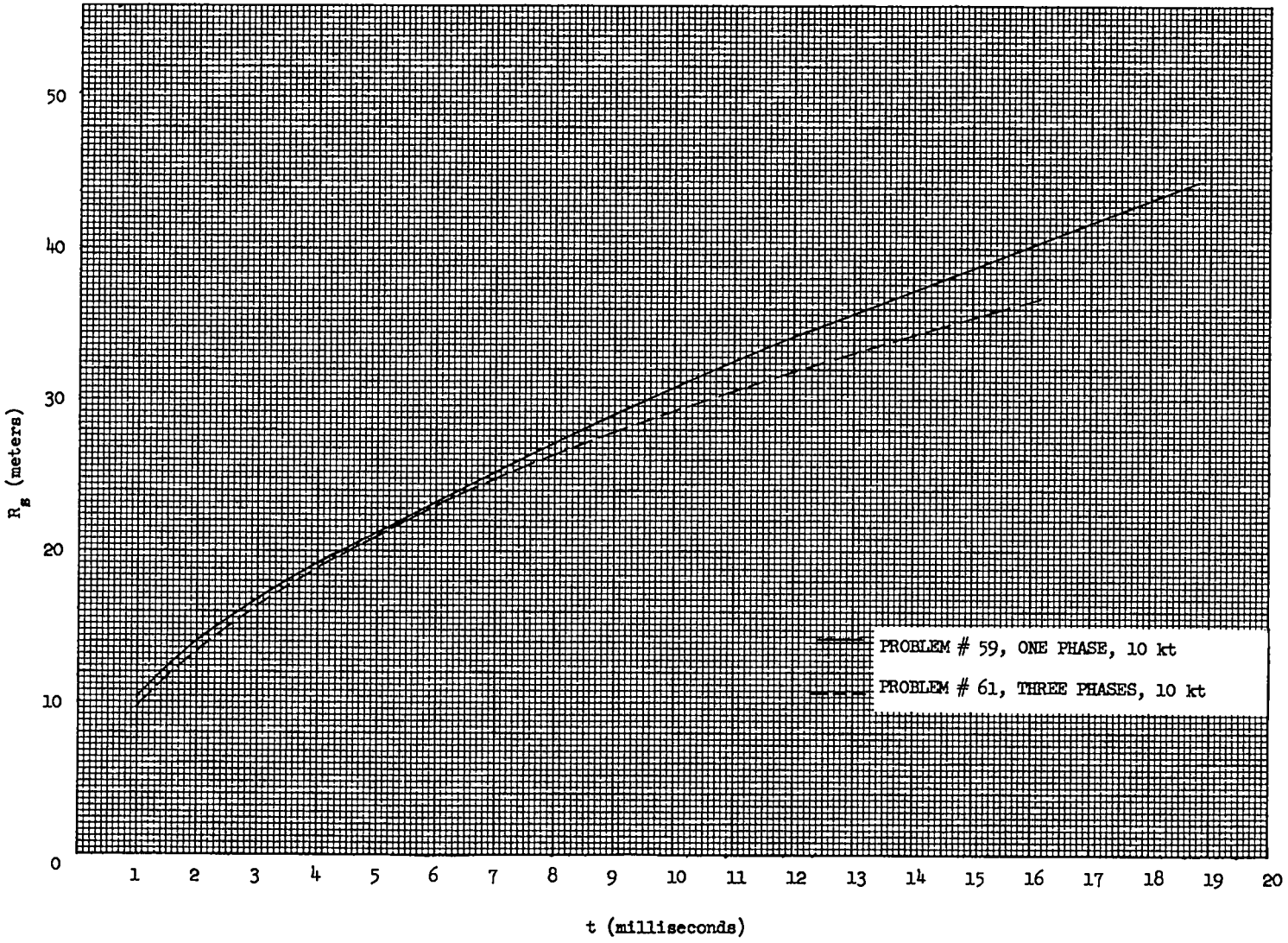


Figure 4

SECRET

SECRET

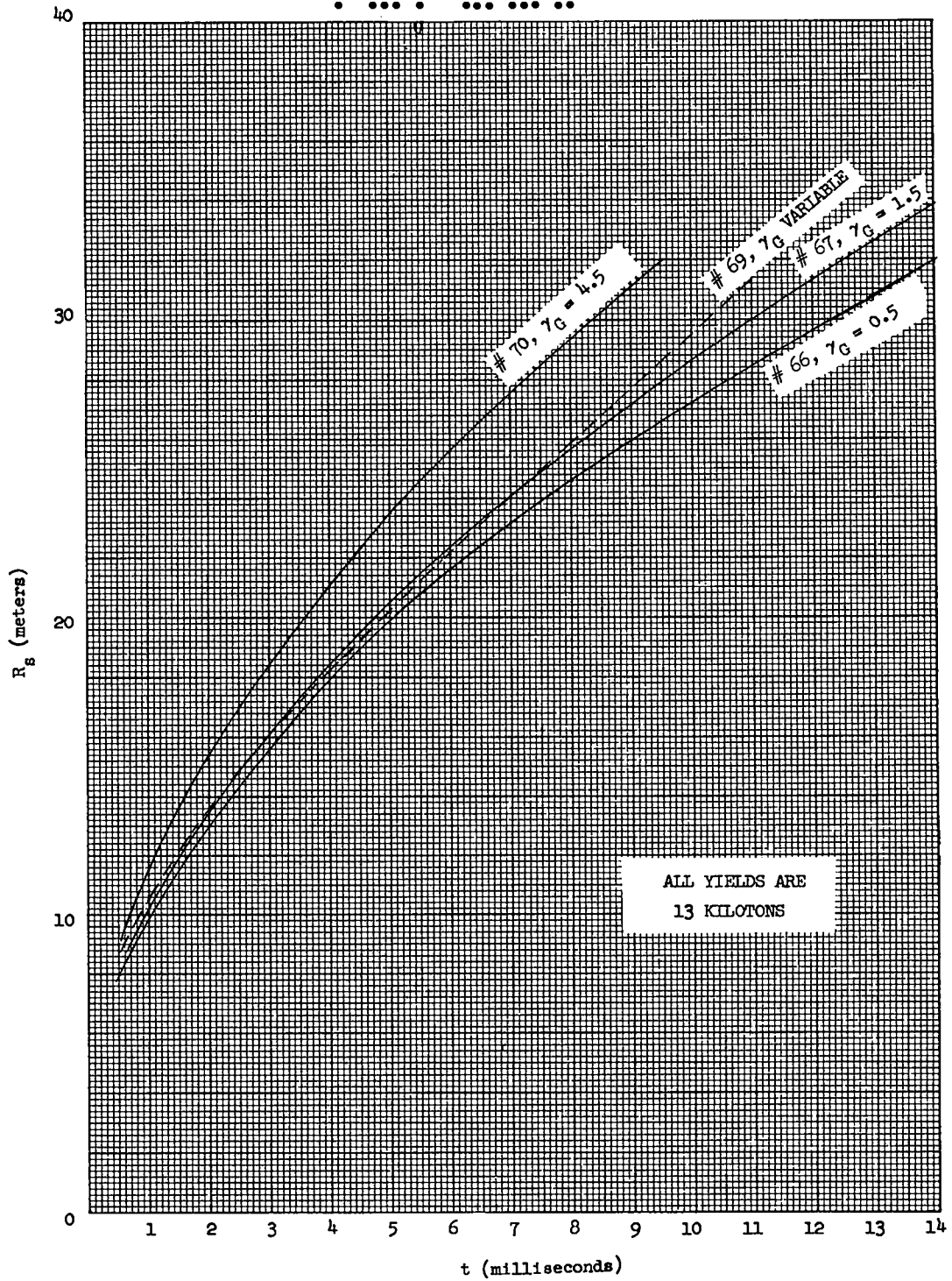


Figure 5

SECRET

SECRET

04170
0370

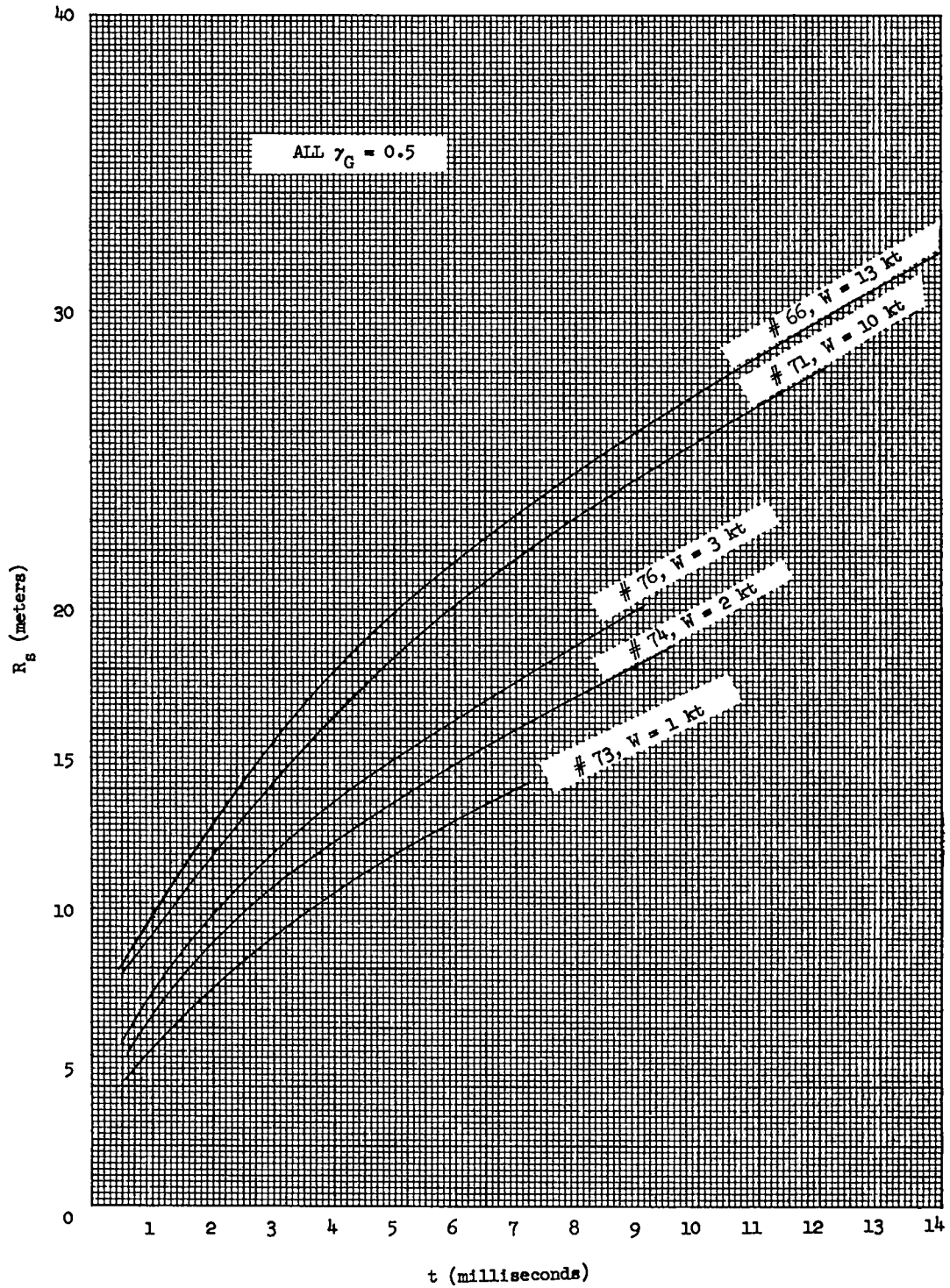


Figure 6

28

04170
0370

UNCLASSIFIED



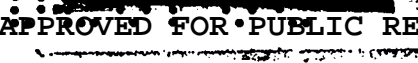


These are the first three phases (except for the sonic precursor) as defined by the GMX-6 data (see solid line in figure 1). Both problems were run with a variable γ_G (equation 11). Figure 4 points up the importance of verifying by static measurements the low pressure extrapolation of the GMX-6 data as was discussed in part II above.

Figure 5 shows the effect of the assumed Grüneisen's ratio. All of these problems were run with the phase constants (20) plus a sonic precursor of 1.5 m/ms up to 1 kb as illustrated in figure 1. All these problems were computed at 13 kt but with constant values of γ_G of 0.5, 1.5 and 4.5. At early times the curves are somewhat insensitive to values of γ_G below about 1.5. The curve for $\gamma_G = 0.01$ (not shown) lies just slightly below that shown for $\gamma_G = 0.5$. It is interesting to see the effect of a variable γ_G (equation 11) in the curve for problem 69. At late times when a large fraction of the material behind the shock has expanded considerably, equation 11 indicates that, on the average, γ_G is quite large behind the shock and this is confirmed by the curve in figure 5. As has been stated above, the Dugdale-MacDonald relation seems of dubious merit when applied to rocks, and we have chosen to make our yield analyses on the basis of a fixed γ_G somewhere in the range 0.5 - 1.5. For example, problem 66 with $\gamma_G = 0.5$ matches the observed points from Fisher shot very well. If the Dugdale-MacDonald relation were used for data analyses, we would have a very difficult time matching the observed points as well as we do by using a fixed γ_G .

Finally, figure 6 shows the computed yield sensitivities for a fixed γ_G of 0.5. All the curves are plotted to times at which the computed pressures at the shock front were of the order of 5 to 10 kb. At later times we would expect to see essentially the sonic precursor whose velocity is independent of yield.





UNCLASSIFIED

UNCLASSIFIED



In view of the uncertainties in the ambient density and Grüneisen's ratio and the computed sensitivities to melting point and zoning differences, it would appear that the yield accuracy obtainable by fitting these curves to observed times of arrival is of the order of $\pm 30\%$.

UNCLASSIFIED

03710

